Available online at www.sciencedirect.com
ScienceDirect
JOURNAL OF RARE EARTHS, Vol. 34, No. 7, July 2016, P. 675
JOURNAL OF RARE EARTHS
www.re-journal.com/en/

Cerium, manganese and cerium/manganese ceramic monolithic catalysts. Study of VOCs and PM removal

COLMAN-LERNER Esteban[1,2,3], PELUSO Miguel Andrés[1,2,*], SAMBETH Jorge[1,2], THOMAS Horacio[1,4]

(1. Centro de Investigación y Desarrollo en Ciencias Aplicadas "Dr. Jorge J. Ronco" CONICET CCT La Plata, UNLP, 47 N° 257 (1900) La Plata, Argentina; 2. Fac. de Ciencias Exactas, UNLP, 47 and 115 (1900) La Plata, Argentina; 3. Centro de Investigaciones del Medio Ambiente (CIMA). Facultad de Ciencias Exactas, UNLP. 47 y 115. 1900 – La Plata; 4. Planta Piloto Multipropósito PLAPIMU, CICPBA-UNLP, C. Centenario and 506, M. B. Gonnet, Argentina)

Received 10 January 2016; revised 5 April 2016

Abstract: Ceramic supported cerium, manganese and cerium-manganese catalysts were prepared by direct impregnation of aqueous precursor, and characterized by scanning electron microscopy (SEM), X-ray diffraction (XRD), Brunauer-Emmett-Teller method (BET), temperature programmed reduction (H_2-TPR), X-ray photoelectron spectroscopy (XPS) acidity measurements and electrical conductivity. The catalytic activity was evaluated for volatile organic compounds (VOC) (ethanol, methyl ethyl ketone and toluene) oxidation. Additionally, catalysts were tested in particulate matter (PM) combustion. The characterization results indicated that Ce was in the form of Ce^{4+} and Ce^{3+}, and Mn existed in the form of Mn^{4+} and Mn^{3+} on the surface of the Mn/AC sample and in the form of Mn^{4+} in the Ce/Mn/AC monolith. VOC oxidation results revealed that the Ce/Mn/AC sample showed an excellent performance compared with ceramic supported CeO_2 (Ce/AC) and MnO_x (Mn/AC) samples. The PM combustion was also higher on Ce/Mn/AC monoliths. The enhanced catalytic activity was mainly attributed to the Ce and Mn interaction which enhanced the acidity, conductivity and the reducibility of the oxides.

Keywords: monolith; VOCs; MnO_x; Ce; PM; clays; rare earths

Volatile organic compounds (VOCs) are important components in the urban environment, arising from natural and anthropogenic processes and commonly present indoors and outdoors. Fifty percent of the total VOCs and more than eighty percent of benzene emissions outdoors are due to vehicle exhaust and evaporative losses. Besides vehicular traffic, emissions from industrial sources, e.g., petroleum refineries and petrochemical plants play an important role in affecting the atmosphere quality[1,2]. The simultaneous reduction in the emission of particulate matter (PM) and volatile organic compounds (VOCs) has been a great challenge for automobile manufacturers and researchers. In fact, in several cases, emissions of volatile organic compounds are accompanied by the emission of carbon particles. The use of catalysts in order to oxidize the carbonaceous particles is one of the promising exhaust gas after treatment systems. These catalysts also provide significant reductions in emissions of carbon monoxide (CO) and hydrocarbons (HC). For diminishing the particulate matter emissions, the catalytic filter that combines soot retention and combustion is one of the most alternatives studied. Noble metals (Pt, Pd) or transition metal based-oxides (cerium oxide) are widely used as active phases[3–5]. Metal oxides have lower activity than noble metal catalysts but they are cheaper and have greater resistance to some poisons. Among the transition metal oxides, manganese and cerium based materials have been considered as promising catalysts for the combustion of VOCs[6].

Manganese oxides are widely used due to their low cost and high activity, which is attributed to the labile lattice oxygen and their capacity of storing oxygen in the crystalline structure[6–8]. Catalysts based on cerium oxides are attracting attention as catalyst for VOCs combustion due to the oxygen vacancies and high surface reducibility produced for the Ce^{4+}/Ce^{3+} redox pair[9,10]. The combination of manganese and cerium could modify the redox properties of the mixed oxides, enhancing the mobility of oxygen and improving the catalytic activity for VOCs combustion[11,12].

The properties of cerium oxides mentioned are responsible for their wide use in the combustion of soot, which is reported to involve a redox cycle where active oxygen species oxidize soot. Doping cerium based catalysts with manganese is often employed to enhance the soot combustion of cerium oxides[10,13].

For environmental applications, high flow rates should be treated and a low-pressure drop is required. For that reason, the catalytic system most widely used for catalytic VOC oxidation is the monolithic reactor[14].

Foundation item: Project supported by National Scientific and Technical Research Council of Argentina (PIP 942) and National Science and Technology Promotion Agency of Argentina (PICT 2012-2366)

* **Corresponding author:** PELUSO Miguel Andrés (**E-mail:** apelu@quimica.unlp.edu.ar; **Tel.:** +54 221 4210711)

DOI: 10.1016/S1002-0721(16)60078-9

Being a better alternative to metallic ones, the rheological properties of clay minerals are ideal raw materials for preparing monoliths[15,16]. Although the most common ceramic supports used is the cordierite, the abundance of natural clay and its low cost are likely to make it candidate as structured catalysts support.

Moreover, the typical method to deposit the catalysts onto the monoliths surface is preparing slurry of an existent powder. The problem of this technique is related to the adherence quality of the layer on the monolithic carrier surface. The use of clays in the formulation of monoliths could produce ceramic (macroporous) structures in which the deposition of the catalyst support can be performed directly by impregnation of aqueous precursors.

In a previous paper[17], we studied the use of Mn, Pt and Pt/Mn supported ceramic monoliths for the combustion of ethanol and toluene. The aim of the present paper was to study the catalytic behavior of Ce and Ce/Mn supported monoliths, in the combustion of ethanol, methyl ethyl ketone (MEK) and toluene. Additionally, the combustion of soot was investigated over the prepared monoliths, in order to study if the Ce-Mn catalysts are active catalyst not only for VOCs elimination but also for particulate matter combustion.

1 Experimental

1.1 Catalyst preparation

The preparation of the ceramic monoliths (denoted as AC) used as support together with the preparation of the Mn supported monoliths (denoted as Mn/AC) were described in a previous paper[17].

Supported Ce and Ce/Mn monoliths were prepared as follows:

Ce/AC: ceramic monoliths (AC) were immersed in an aqueous solution of 0.02 mol/L $Ce(NO_3)_3$, inside a closed vessel and put through to mechanical orbital agitation for 60 min.

Ce/Mn/AC: Mn/AC monoliths, after having been calcined at 500 ºC, were impregnated with 0.02 mol/L $Ce(NO_3)_3$ in the same way as the Ce/AC monoliths. After impregnation, monoliths were washed with deionized water, dried overnight at 100 ºC and finally calcined at 500 ºC for 2 h.

1.2 Catalyst characterization

Textural properties of the monoliths were determined by nitrogen adsorption using a Micromeritics ASAP 2000 sorptometer. The experiments were performed over small pieces of crushed monoliths.

The sample morphology was examined with a scanning electron microscope (SEM) Philips SEM 505. The experiments were performed over small pieces of crushed monoliths.

X-ray diffraction patterns were carried out at room temperature with a Phillips PW1390 instrument by using Ni filter and Cu Kα radiation (λ=0.1540589 nm) in the 2θ range between 5º and 70º, at 0.02(º)/min scanning speed and a counting time of 2 s per step. The samples were measured in powder form (previously ground monolith).

X-ray photoelectron spectra (XPS) of the samples were obtained (over previously ground monolith in powder form) using a multi-technique system, equipped with a hemi-spherical PHOIBOS 150 analyzer using Mg X-ray source. Binding energies (BE: ±0.1 eV) were calculated using adventitious hydrocarbon (C 1s=284.6 eV) as the internal reference. Curve fitting was performed with the CasaXPS program (Casa Software Ltd., UK).

The temperature-programmed reduction (TPR) with hydrogen was performed using a Quantachrome equipment Quantasorb Jr. The experiments were carried out at a heating rate of 10 ºC/min. The reactive gas composition was H_2 (5 vol.%) in nitrogen. The flow rate was fixed at 22 cm^3/min. Temperature was increased from ambient to 900 ºC. The H_2 consumption was measured by a thermal conductivity detector, and the H_2 uptakes were quantified using CuO as a standard and taking into account that at the end of the experiments all Mn is as MnO.

Acidity of the monoliths was measured in a Metrohm 794 Basic Titrino with interchanged unity 806 and a Metrohm electrode. A representative 0.50 g sample in powder form was suspended in 45 mL of acetonitrile solution and allowed 3 h in agitation to come to stabilization. This suspension was then titrated with 0.025 N n-butylamine solution.

The electrical conductivity of the monoliths was estimated measuring the electrical resistance in a SIEMENS ISOWID B4105 Insulation Tester, applying 500v among the monoliths. The conductivity was calculated as the inverse of the resistance.

1.3 Catalytic oxidation of VOCs

The catalytic activity of the prepared monoliths was measured for the complete oxidation of three different VOCs: ethanol, MEK and toluene. VOC oxidation was carried out in a stainless steel tubular fixed-bed reactor of 45 cm high and 2.3 cm in inner diameter, under atmospheric pressure at a space velocity of 12000 h^{-1}. The reactive flow (1000 cm^3/min) was composed of air and 1000 mgC/m^3 of gaseous VOC. Monolith was placed on the top of a carborundum bed. The reactor was surrounded by an electrical furnace equipped with three independent temperature programmers. The ignition curves were obtained over the range 100–500 ºC in incremental steps (25 ºC) and the reaction temperature was measured by a thermocouple placed in the middle of the monolith. The data were obtained in steady state. Monoliths were treated under 1000 cm^3/min of air at 450 ºC for 1 h before reaction, and then cooled down in air to the starting

reaction temperature. VOC conversion in the effluent gas was analyzed by on-line Gas Chromatography (Shimadzu GC9A), together with the CO_2 measurement by an on-line IR detector (Telaire T6613). The yield to CO_2 was calculated as the ratio between the CO_2 concentrations divided by its value measured when complete conversion at high temperature had been reached. In ethanol oxidation, acetaldehyde yield was calculated as moles of ethanol converted to acetaldehyde divided by the moles of ethanol fed into the reactor.

1.4 PM combustion

The catalytic activity of the prepared monoliths towards PM combustion was carried out by temperature programmed oxidation (TPO) using the same apparatus as the one described above. Before tests, the monoliths were washcoated with a 10 wt.% suspension of carbon black (CB) in ethanol. Monoliths were dipped into the slurry for 30 s, withdrawn to constant speed of 3 cm/min and then, the suspension excess was eliminated by centrifugation at 400 r/min for 10 min. Finally, they were dried at 120 ºC for 1 h. Three immersions were performed. After impregnation, the loading of soot was gravimetrically determined. A loose contact was obtained with this impregnation method[18].

CB-monoliths were placed in the reactor and heated from room temperature to 500 ºC (25 ºC/min) in air flow (1000 cm^3/min). The combustion was followed by CO_2 measurement by an on-line IR detector (Telaire T6613).

2 Results

2.1 Catalyst characterization

The specific area along with the percentage of Mn and Ce determined by XPS of the samples used are listed in Table 1. The addition of Ce and or Mn has no significant effect on the specific area of the support.

Fig. 1(a–d) shows the SEM micrographs of prepared monoliths. In the solid Mn/AC there is a cluster of small surface particles on the support matrix. The MnO_x layer is deposited on the support surface changing its mor-

Table 1 Properties of monoliths

Monolith	Ce content/%	Mn content/%	S_{BET}/(m^2/g)	Conductivity/(S/cm)	ΔE_s Mn 3s	Mn AOS
AC			53	1.5×10^{-4}		
Mn/AC		1.5	56	2.6×10^{-4}	4.8	3.6
Ce/AC	0.3		57	4.8×10^{-4}		
Ce/Mn/AC	0.2	1.4	54	5.5×10^{-4}	4.5	3.9

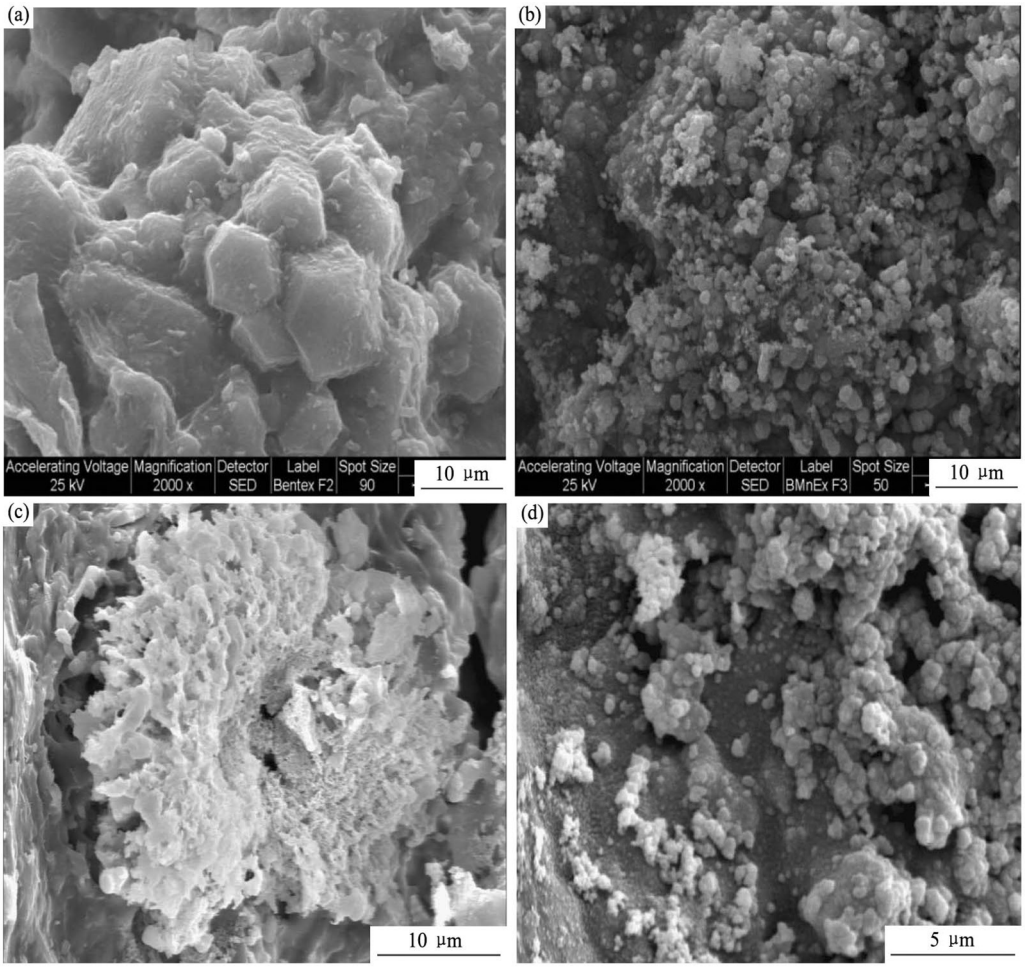

Fig. 1 SEM micrographs of pieces of monoliths
(a) AC; (b) Mn/AC; (c) Ce/AC; (d) Ce/Mn/AC

phology. Ce/Mn/AC presents globular particles. In the case of Ce/AC, the surface presents cracks and holes.

Results of the data of conductivity per cm of the monoliths (conductivity along the length of the monolith) are presented in Table 1. The order of conductivity was Ce/Mn/AC>Mn/AC>Ce/AC>CM. The increase in the conductivity of the Ce/Mn/AC monolith is associated to the Ce-Mn interaction. Similar conclusion were reported by Gebhardt et al.[19], Balducci et al.[20], D´Alessandro et al.[21] and Wang et al.[22] who have reported theoretically and experimentally that the presence of Ce and Mn modified the electrical properties from the strong interaction.

The XRD spectra of the monoliths are presented in Fig. 2. The X-ray diffraction pattern of the bare monolith shows the diffraction lines corresponding to the support, Al_2O_3, SiO_2 and bentonite. Mn/AC, Ce/AC and Ce/Mn/AC samples also present the diffraction lines of the support. Additionally, small peaks corresponding to $K_{0.7}MnO_2$ (JCPDS 31-1052) were detected in Mn/AC and Ce/Mn/AC catalysts. On the other hand, CeO_2 (JCPDS 81-0792) was detected in the samples containing cerium.

The oxidation state of catalyst surface species was examined by XPS analysis.

Results are presented in Fig. 3. For Mn/AC catalyst, the Mn $2p_{3/2}$ spectral shape could be reproduced with two Mn $2p_{3/2}$ components at 641.1 and 643.1 eV assigned to Mn^{3+} and Mn^{4+}, respectively[23]. In the Ce/Mn/AC catalysts the Mn $2p_{3/2}$ peak is deconvoluted in one single peak centered at 642.3 eV assigned to Mn^{4+}. Note that the Mn $2p_{3/2}$ binding energy of the Ce/Mn/AC catalyst is lower than those of the pure Mn/AC, which indicates a strong interaction between manganese and cerium[24].

It is well known that for manganese oxides it is insufficient to employ the BE shifts of the Mn $2p_{3/2}$ to clearly distinguish the various manganese species (Mn^{2+}, Mn^{3+} and Mn^{4+}). As an alternative, the magnitude of Mn 3s multiplet splitting can be used to calculate the average oxidation state (AOS) of manganese, according to the following relationship[25]

$$AOS=8.95–1.13\Delta E_s \text{ (eV)} \quad (1)$$

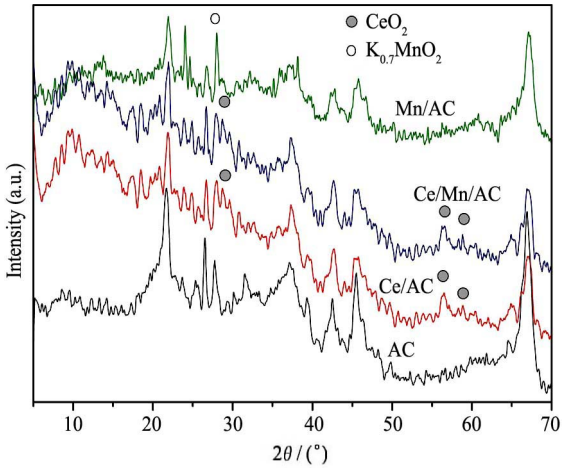

Fig. 2 X-ray diffraction patterns of samples

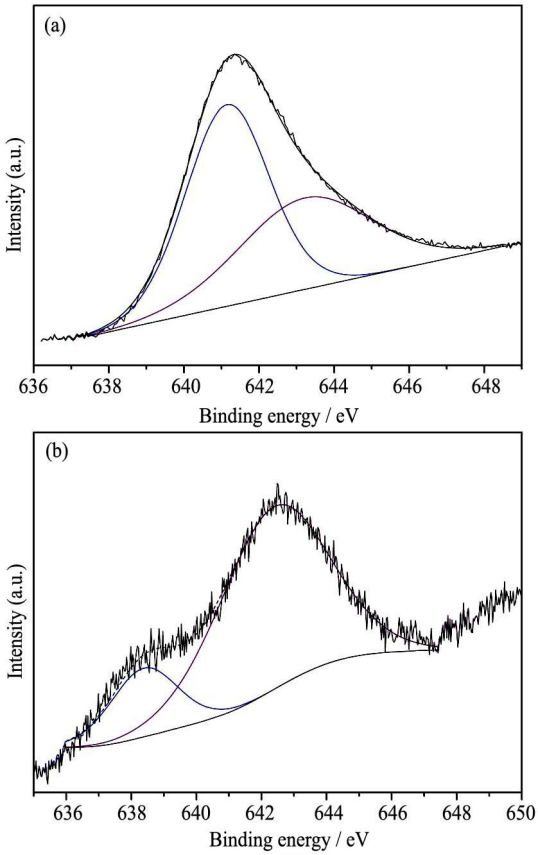

Fig. 3 XPS spectra of Mn 2p region
(a) Mn/AC; (b) Ce/Mn/AC

where ΔE_s represents the multiplet splitting, which is the energy difference between the main peak and its satellite. Results are listed in Table 1.

It has been seen that in the Mn/AC sample, manganese is present in the mixed valence Mn^{3+} and Mn^{4+} state, whereas in the Ce/Mn/AC manganese is present only as Mn^{4+}, which is coincident with the results of Li et al.[26].

The XPS spectra of Ce 3d in the Ce/AC and Ce/Mn/AC samples are represented in Fig. 4. The spectra were deconvoluted into two spin-orbit, and letters U and V refer to the $3d_{3/2}$ and $3d_{5/2}$ spin-orbit components respectively[26,27]. The peaks V, V^{II}, V^{III}, U, U^{II} and U^{III} were attributed to Ce^{4+} [28]. The U^{I} peak is assigned to Ce^{3+} [29]. XPS results confirm that Ce^{4+} and Ce^{3+} coexist on the surface of catalysts.

The redox properties of monoliths were investigated using the H_2-TPR technique. The corresponding TPR profiles are shown in Fig. 5. Taking into account that alumina and silica do not show any hydrogen consumption in the investigated temperature, the reduction peaks observed can be attributed to manganese or cerium species. Ce/AC monoliths presents a peak centered at 550 ºC, associated to the reduction of CeO_2[30]. In Mn/AC sample, a shoulder at lower temperature (310 ºC) is related to the reduction of highly dispersed MnO_x species[31–33]. The two reduction peaks observed at ~409 and 495 ºC corresponded to the combined reduction of MnO_2 or Mn_2O_3

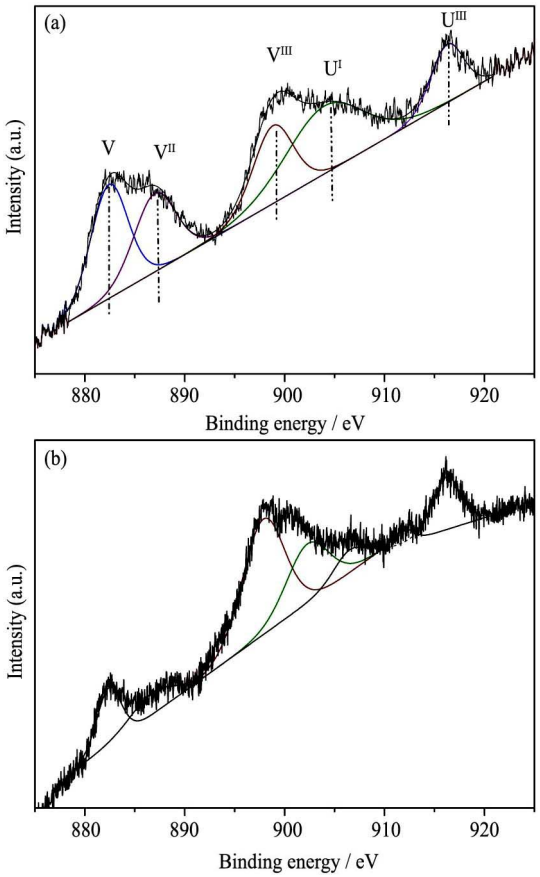

Fig. 4 XPS spectra of Ce 3d region
(a) Ce/AC; (b) Ce/Mn/AC

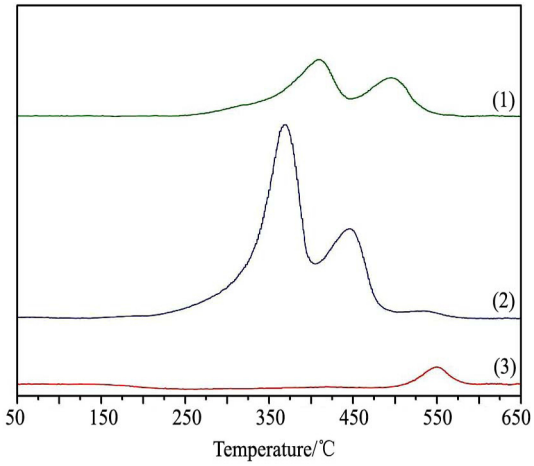

Fig. 5 H_2-TPR patterns of monoliths
(1) Mn/Ac; (2) Ce/Mn/AC; (3) Ce/AC

to Mn_3O_4[34], and to the reduction of Mn_3O_4 to MnO or the reduction of Mn_5O_8 to MnO[35], respectively. On the other hand, the TPR profile of the Ce/Mn/AC sample shows three reduction peaks. The first reduction peak at ~367 ºC can be due to the successive reduction of readily reducible manganese species (Mn^{4+} and/or Mn^{3+}). The second peak at ~446 ºC can be attributed to the reduction of Mn_3O_4 to MnO together with the reduction of surface $Ce^{4+}\rightarrow Ce^{3+}$. The highest temperature peak at ~531 ºC could be associated to the reduction of bulk CeO_2 and then formation of Ce_2O_3. The reduction peaks in Ce/Mn/AC sample are shifted towards lower temperatures, which reflected the increase of oxygen mobility and it can be due to a synergistic interaction between highly dispersed CeO_2 and MnO_x over the support[24,36]. Taking into account the H_2 consumption in the samples, a manganese average oxidation state (AOS) of 3.6 and 3.9 was calculated for Mn/AC and Ce/Mn/AC, respectively.

The results of electrical conductivity and H_2-TPR are a clear evidence of the interaction between manganese and cerium, which are associated with the reducibility at low temperature of manganese oxides and the mobility of oxygen species.

The acidity of the samples was measured by titration with n-butylamine. Results are presented in Fig. 6. Additionally, the different types of acid sites are presented in Table 2. They were calculated from the area under the curve which is proportional to the numbers of acid sites. The impregnation of the support with manganese or cerium generates strong acid sites. The order of strong acid sites was: Ce/Mn/AC>Mn/AC>Ce/AC. The Ce-Mn interaction favors the formation of acid sites, which could be associated to Bronsted species, in accord with Rey-Bueno et al.[37].

2.2 VOC oxidation

The catalytic performance of the prepared monoliths was evaluated in the oxidation of three different VOCs: ethanol, methyl ethyl ketone and toluene.

Fig. 7(a) shows the light-off curves for ethanol oxidation. It was plotted that the CO_2 was yielded as a function of reaction temperature. There are no significant differences in the catalytic activity of the Mn/AC and Ce/AC

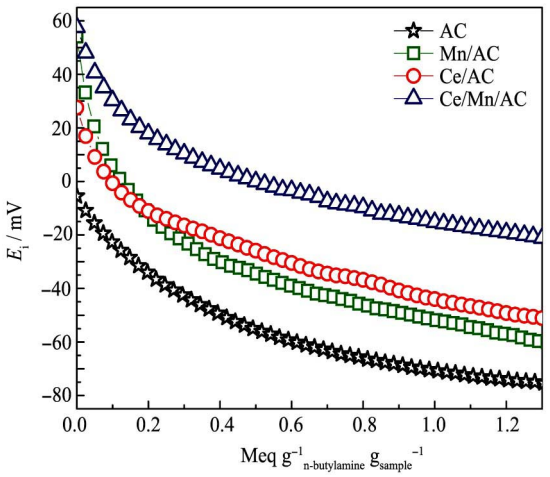

Fig. 6 Titration of samples with n-butylamine

Table 2 Acid sites

Monolith	E_i/ mV	Total area/ (mV/Meq/g)	Strong acid sites/%	Weak acid sites/%
AC	0	39	0	100
Mn/AC	60	37	9	91
Ce/AC	30	32	5	95
Ce/Mn/AC	60	24	63	37

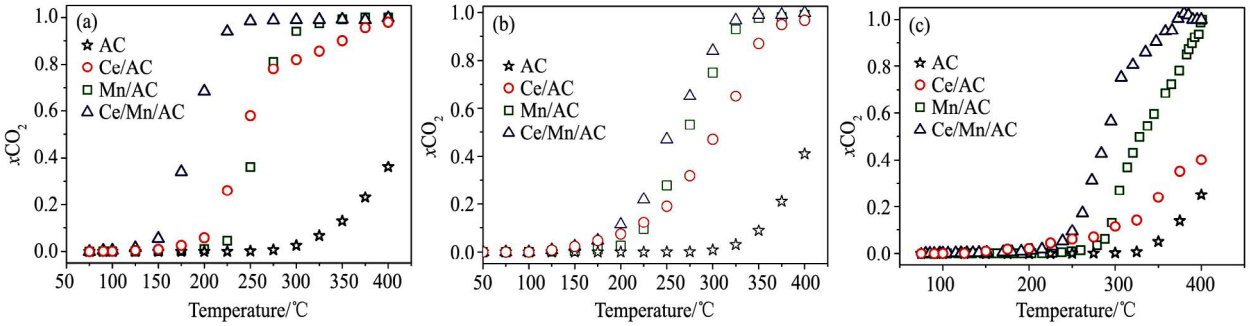

Fig. 7 CO_2 yield in ethanol combustion (a), MEK combustion (b) and toluene combustion (c)

monoliths. Ce/Mn/AC presents higher ethanol conversion, with a T_{50} and T_{90} (temperature at 50% and 90% conversion, respectively) lower to about 65 ºC than the other catalysts.

In the case of MEK total oxidation (Fig. 7(b)), the addition of Ce to Mn/AC improves the activity but in a less extent than in the oxidation of ethanol. All catalysts are less active in MEK oxidation and complete conversion to CO_2 takes place at temperatures higher by 20 ºC compared to ethanol.

In Fig. 7(c) the light-off curves relative to toluene combustion on the monoliths are compared. Ce/Mn/AC is definitely the most active one, showing high toluene conversion (80 %) at 300 ºC, while at this temperature Ce/AC catalyst is slightly active. The activity sequence is clearly Ce/Mn/AC>Mn/AC>Ce/AC. As in the case of ethanol oxidation, the addition of Ce to Mn enhanced toluene conversion, lowering the T_{50} and T_{90} to about 50 and 60 ºC, respectively. Toluene is most resistant to oxidation among the three VOCs examined and complete conversion is achieved at 370 ºC over the Ce/Mn/AC monolith.

In toluene oxidation, the only product was CO_2 at all conversion levels, and no formation of by-products was detected. In the case of MEK oxidation, only small traces of acetaldehyde were detected at low levels of conversions.

In ethanol oxidation, acetaldehyde was also detected. However, as can be seen in Fig. 8, the yield did not exceed 8% for Ce/Mn/AC and Ce/AC, and it is negligible for Mn/AC monolith. The maximum of acetaldehyde occurs at around 200 and 275 ºC for Ce/Mn/AC and Ce/AC, respectively.

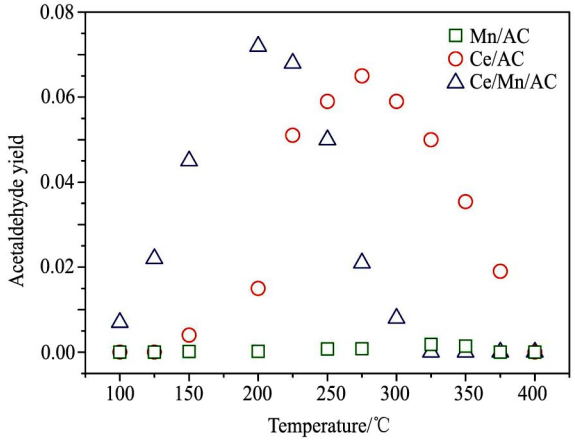

Fig. 8 Evolution of acetaldehyde yield with reaction temperature in ethanol combustion

In accord with the TPR results, the reduction of the Mn/AC catalyst occurs at higher temperatures than in Ce/Mn/AC, and consequently the oxidation of VOCs on the Mn/AC catalyst was more difficult than that on the Ce/Mn/AC catalyst[36].

Additionally, VOCs conversion in this work depends on the acidity of the samples, the more the acidity of the samples, the more the VOC conversion.

It is widely accepted in the literature that both these catalytic properties, acidity and reducibility, are closely related to an efficient hydrocarbon destruction[38]. Several authors observed an increase in the oxidation capacity of VOCs when the acidity of the catalysts increases[39–41].

The electrical conductivity of the samples is correlated to the conversion of VOCs. The Volkenshtein Electronic Theory[42] states that the catalytic activity is a function of the electronic properties of solids. The electrical conductivity of the samples prepared in this work increases in the same way that increases the VOC conversion.

The increased electrical conductivity of the Ce/Mn/AC monolith could be due to a favorable synergetic effect between Ce and Mn, which is responsible for the higher activity of the Ce/Mn/AC catalyst.

2.3 Particulate matter combustion

Temperature-programmed oxidation experiments were carried out in order to study the ceramic monoliths in the soot combustion reaction. Soot was incorporated onto the monoliths using carbon black suspensions as described in the experimental section. TPO profiles are shown in Fig. 9. The results show that the incorporation of metals onto the ceramic monoliths decreases the temperature at which the CO_2 production rate was maximum, from 460 to 350 ºC, for the most active catalyst. For the four monoliths studied, the temperature of the maximum of CO_2 increases in the order: Ce/Mn/AC<Mn/AC<Ce/AC <CM. These results are coincident to that obtained for VOCs combustion. It is generally known that the catalytic activities of the catalysts for soot combustion are closely related to their redox properties[43]. Ceria-based

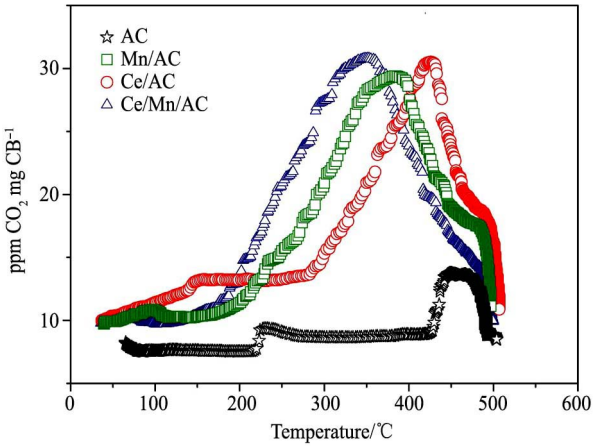

Fig. 9 Soot combustion over monoliths

materials present good catalytic performance as soot combustion catalysts, due to the ability of cerium to switch between the Ce^{4+} and Ce^{3+} oxidation states and to incorporate more or less oxygen into the crystal structure. Manganese oxides with different oxidation states (cryptomelane, Mn_3O_4) are also as active as soot combustion Pt catalysts[44,45]. Among the prepared catalysts Ce/Mn shows better redox property than the pure Ce and Mn catalysts, and consequently, the active oxygen species on the surface of the catalyst may show strong property for the soot oxidation, in accord with several authors[46,47].

The studies carried out in this work demonstrated that the Ce/MnO_x active phase supported on ceramic monolith is a promising catalyst for VOCs and PM abatement. Further investigation in different shapes and different materials for monolith supports is currently being carried out in our laboratory.

3 Conclusions

Mn, Ce and Ce/Mn supported ceramic monoliths using natural clays as raw materials were prepared. The impregnated phases showed excellent adhesion to the monoliths. The addition of Ce to Mn facilitated the reduction of the manganese oxide phases and increased the electrical conductivity and the surface acidity of the sample.

The conversion of ethanol, MEK and toluene was higher on Ce/Mn/AC.

In the soot combustion, the lower temperature of evolved CO_2 was also on the Ce/Mn/AC.

The synergetic effect between Ce and Mn promoted redox behavior, higher conductivity and surface acidity, and played an important role in the complete catalytic oxidation of VOCs and soots.

Acknowledgements: Authors would like to express thanks to Dra. I. Lick, Ing. E. Soto, M. Theiller and Tco. L. Osiglio.

References:

[1] Colman-Lerner J E, Kohajda T, Aguilar M E, Massolo L A, Sánchez E Y, Porta A A, Opitz P W, Gunnar H, Olf M. Improvement of health risk factors after reduction of VOC concentrations in industrial and urban areas. *Environ. Sci. Pollut. Res*., 2014, **21**(16): 9676.

[2] IARC Working Group on the Evaluation of Carcinogenic Risks to Humans. Chemical Agents and Related Occupations, 2012.

[3] Alifanti M, Florea M, Somacescu S, Parvulescu V I. Supported perovskites for total oxidation of toluene. *Appl. Catal. B*, 2005, **60**(1-2): 33.

[4] Peluso M A, Gambaro L A, Pronsato E, Gazzoli D, Thomas H J, Sambeth J E. Synthesis and catalytic activity of manganese dioxide (type OMS-2) for the abatement of oxygenated VOCs. *Catal. Today*, 2008, **133-135**(1-4): 487.

[5] Li T, Lei Y, He Y M, Teng B T, Luo M F, Zhao L H. Catalytic combustion of toluene on Pd/$Ce_xLa_{1-x}O_2$/monolith catalysts. *React. Kinet. Mech. Catal*., 2011, **103**(2): 419.

[6] Craciun R. Structure and redox properties of MnO_x/yttrium-stabilized zirconia (YSZ) catalyst and its used in CO and CH_4 oxidation. *Appl. Catal. A*, 2003, **243**(1): 67.

[7] Luo J, Zhang Q H, Huang A M, Suib S L. Total oxidation of volatile organic compounds with hydrophobic cryptomelane-type octahedral molecular sieves. *Microporous Mesoporous Mater*., 2000, **35-36**: 209.

[8] Tang X F, Xu Y D, Shen W J. Promoting effect of copper on the catalytic activity of MnO_x-CeO_2 mixed oxide for complete oxidation of benzene. *Chem. Eng. J*., 2008, **144**(2): 175.

[9] Ivanova A S. Physicochemical and catalytic properties of systems based on CeO_2. *Kinet. Catal*., 2009, **50**(6): 797.

[10] Liu S, Wu X D, Weng D, Ran R. Ceria-based catalysts for soot oxidation: a review. *J. Rare Earths*, 2015, **33**(6): 567.

[11] Delimaris D, Ioannides T. VOC oxidation over MnO_x-CeO_2 catalysts prepared by a combustion method. *Appl. Catal. B*, 2008, **84**(1-2): 303.

[12] Picasso G, Cruz R, Sun Kou M D R. Preparation by coprecipitation of Ce–Mn based catalysts for combustion of n-hexane. *Mater. Res. Bull*., 2015, **70**: 621.

[13] Fu M L, Lin J M, Zhu W B, Wu J L, Chen L M, Huang B C, Ye D Q. Surface reactive species on $MnO_{x(0.4)}$-CeO_2 catalysts towards soot oxidation assisted with pulse dielectric barrier discharge. *J. Rare Earths*, 2014, **32**(2): 153.

[14] Avila P, Montes M, Miró E E. Monolithic reactors for environmental applications. *Chem. Eng. J*., 2005, **109**(1-3): 11.

[15] Benbow J, Bridgwater J. Paste Flow and Extrusion. Oxford: Oxford University Press, 1993.

[16] Komova O V, Simakov A V, Kovalenko G A, Rudina N A, Chuenko T V, Kulikovskaya N A. Formation of a nickel catalyst on the surface of aluminosilicate supports for the synthesis of catalytic fibrous carbon. *Kinet. Catal*., 2007, **48**(6): 803.

[17] Colman-Lerner J E, Peluso M A, Sambeth J E, Thomas H J. Volatile organic compound removal over bentonite-supported Pt, Mn and Pt/Mn monolithic catalysts. *React. Kinet. Mech. Catal*., 2013, **108**(2): 443.

[18] Neyertz C A, Banús E D, Miró E E, Querini C A. Potassium-promoted $Ce_{0.65}Zr_{0.35}O_2$ monolithic catalysts for diesel soot combustion. *Appl. Catal. A: Gen*., 2014, **474**: 168.

[19] Gebhardt J R, Roy S, Ali N. Colossal magnetoresistance in Ce doped manganese oxides. *J. Appl. Phys*., 1999, **85**(8): 5390.

[20] Balducci G, Islam M S, Kašpar J, Fornasiero P, Graziani M. Reduction process in CeO_2-MO and CeO_2-M_2O_3 mixed oxides: A computer simulation study. *Chem. Mater*., 2003, **15**(20): 3781.

[21] DÁlessandro O, Pintos D G, Juan A, Irigoyen B, Sambeth J. A DFT study of phenol adsorption on a low doping Mn-Ce composite oxide model. *Appl. Surf. Sci*., 2015, **359**: 14.

[22] Wang Y, Liu H, Hu P P, Huang Z W, Gao J Y, Xu F, Ma Z, Tang X F. Enhancing the catalytic activity of Hollandite manganese oxide by supporting sub-10 nm ceria particles. *Catal. Lett.*, 2015, **145**(10): 1880.

[23] Ponce S, Peña M, Fierro J L. Surface properties and catalytic performance in methane combustion of Sr-substituted lanthanum manganites. *Appl. Catal. B*, 2000, **24**(3-4): 193.

[24] Venkataswamy P, Jampaiah D, Lin F, Alxneit I, Reddy B M. Structural properties of alumina supported Ce-Mn solid solutions and their markedly enhanced catalytic activity for CO oxidation. *Appl. Surf. Sci*., 2015, **349**: 299.

[25] Galakhov V R, Demeter M, Bartkowski S, Neumann M, Ovechkina N A, Kurmaev E Z, Lobachevskaya N I, Mukovskii Y, Mitchell J, Ederer D L. Mn 3s exchange splitting in mixed-valence manganites. *Phys. Rev. B*, 2002, **65**: 113102.

[26] Li L, Diao Y F, Liu X. Ce-Mn mixed oxides supported on glass-fiber for low-temperature selective catalytic reduction of NO with NH_3. *J. Rare Earths*, 2014, **32**(5): 409.

[27] Anandan C, Bera P. XPS studies on the interaction of CeO_2 with silicon in magnetron sputtered CeO_2 thin films on Si and Si_3N_4 substrates. *Appl. Surf. Sci*., 2013, **283**: 297.

[28] Wu Y S, Zhang Y X, Liu M, Ma Z C. Complete catalytic oxidation of o-xylene over Mn-Ce oxides prepared using a redox-precipitation method. *Catal. Today*, 2010, **153**(3-4): 170.

[29] Mullins D R, Senanayake S D, Chen T L. Adsorption and reaction of C1-C3 alcohols over CeO_x (111) thin films. *J. Phys. Chem. C*, 2010.

[30] Markaryan G, Ikryannikova L, Muravieva G, Turakulova A, Kostyuk B, Lunina E, Lunin V, Zhilinskaya E, Aboukais A. Red-ox properties and phase composition of CeO_2-ZrO_2 and Y_2O_3-CeO_2-ZrO_2 solid solutions. *Colloids Surf. A*, 1999, **151**(3): 435.

[31] Morales M R, Barbero B P, Lopez T, Moreno A, Cadús L E. Evaluation and characterization of Mn-Cu mixed oxide catalysts supported on TiO_2 and ZrO_2 for ethanol total oxidation. *Fuel*, 2009, **88**(11): 2122.

[32] Trawczyński J, Bielak B, Miśta W. Oxidation of ethanol over supported manganese catalysts - Effect of the carrier. *Appl. Catal. B*, 2005, **55**(4): 277.

[33] Liu X S, Lu J Q, Qian K, Huang W X, Luo M F. A comparative study of formaldehyde and carbon monoxide complete oxidation on MnO_x-CeO_2 catalysts. *J. Rare Earths*, 2009, **27**(3): 418.

[34] Gil A, Gandía L M, Korili S A. Effect of the temperature of calcination on the catalytic performance of manganese- and samarium-manganese-based oxides in the complete oxidation of acetone. *Appl. Catal. A,* 2004, **274**(1-2): 229.

[35] Mirzaei A, Shaterian H, Kaykhaii M. The X-ray photoelectron spectroscopy of surface composition of aged mixed copper manganese oxide catalysts. *Appl. Surf. Sci*., 2005, **239**(2): 246.

[36] Tang W X, Wu X F, Liu G, Li S D, Li D Y, Li W H, Chen Y F. Preparation of hierarchical layer-stacking Mn-Ce composite oxide for catalytic total oxidation of VOCs. *J. Rare Earths*, 2015, **33**(1): 62.

[37] del Rey-Bueno F, García-Rodríguez A, Mata-Arjona A, del Rey-Pérez-Caballero F J, Villafranca-Sánchez E. Surface properties and porous texture of montmorillonite-(Ce or Zr) phosphate cross-linked compounds. *Appl. Surf. Sci*., 1997, **120**(3-4): 340.

[38] Gutiérrez-Ortiz J I, de Rivas B, López-Fonseca R, Martín S, González-Velasco J, Rivas B, Gutie J, Gonza J, Martı S. Structure of Mn-Zr mixed oxides catalysts and their catalytic performance in the gas-phase oxidation of chlorocarbons. *Chemosphere*, 2007, **68**(6): 1004.

[39] Soylu G, Özçelik Z, Boz İ. Total oxidation of toluene over metal oxides supported on a natural clinoptilolite-type zeolite. *Chem. Eng. J*., 2010, **162**(1): 380.

[40] Piumetti M, Fino D, Russo N. Mesoporous manganese oxides prepared by solution combustion synthesis as catalysts for the total oxidation of VOCs. *Appl. Catal. B*, 2015, **163**: 277.

[41] Carabineiro S A, Chen X, Konsolakis M, Psarras A, Tavares P, Órfão J, Pereira M, Figueiredo J. Catalytic oxidation of toluene on Ce–Co and La–Co mixed oxides synthesized by exotemplating and evaporation methods. *Catal. Today*, 2015, **244**: 161.

[42] Volkenshtein F F. The Electronic Theory of Catalysis on Semiconductors. Übersetzung aus dem Russischen von N G Anderson. Pergamon Press, Oxford, London, New York, Paris 1963.

[43] Wei Y C, Zhao Z, Jiao J Q, Liu J, Duan A J, Jiang G Y. Preparation of ultrafine Ce-based oxide nanoparticles and their catalytic performances for diesel soot combustion. *J. Rare Earths*, 2014, **32**(2): 124.

[44] Bueno-López A. Diesel soot combustion ceria catalysts. *Appl. Catal. B*, 2014, **146**: 1.

[45] Atribak I, Bueno-López A, García-García A, Navarro P, Frías D, Montes M. Catalytic activity for soot combustion of birnessite and cryptomelane. *Appl. Catal. B*, 2010, **93**(3-4): 267.

[46] Ito K, Kishikawa K, Watajima A, Ikeue K, Machida M. Soot combustion activity of NO_x-sorbing Cs-MnO_x-CeO_2 catalysts. *Catal. Commun*., 2007, **8**(12): 2176.

[47] Muroyama H, Asajima H, Hano S, Matsui T, Eguchi K. Effect of an additive in a CeO_2-based oxide on catalytic soot combustion. *Appl. Catal. A*, 2015, **489**: 235.